Masses, Deformations and Charge Radii—Nuclear Ground-State Properties in the Relativistic Mean Field Model

Lisheng GENG,[1,2,*] Hiroshi TOKI[1,**] and Jie MENG[2,***]

[1]*Research Center for Nuclear Physics (RCNP), Osaka University, Ibaraki 567-0047, Japan*
[2]*School of Physics, Peking University, Beijing 100871, P. R. China*

We perform a systematic study of the ground-state properties of all the nuclei from the proton drip line to the neutron drip line throughout the periodic table employing the relativistic mean field model. The TMA parameter set is used for the mean-field Lagrangian density, and a state-dependent BCS method is adopted to describe the pairing correlation. The ground-state properties of a total of 6969 nuclei with $Z, N \geq 8$ and $Z \leq 100$ from the proton drip line to the neutron drip line, including the binding energies, the separation energies, the deformations, and the rms charge radii, are calculated and compared with existing experimental data and those of the FRDM and HFB-2 mass formulae. This study provides the first complete picture of the current status of the descriptions of nuclear ground-state properties in the relativistic mean field model. The deviations from existing experimental data indicate either that new degrees of freedom are needed, such as triaxial deformations, or that serious effort is needed to improve the current formulation of the relativistic mean field model.

§1. Introduction

The relativistic mean field (RMF) model has achieved great success during the last twenty years.[1)] Starting from an effective Lagrangian density, the nucleons are described as structureless point particles moving independently in the nuclear potential generated by exchanging various mesons, including the isoscalar-scalar σ meson, the isoscalar-vector ω meson, the isovector-vector ρ meson and the photon. Using the classical variational principle, one can obtain the Dirac equations for nucleons and the Klein-Gordon equations for mesons. These equations are very difficult to solve, and for this reason, usually two simplifications have to be made in any practical application, i.e. the mean-field approximation and the no-sea approximation. The mean-field approximation treats the meson fields as classical c-numbers, and the no-sea approximation implies that the vacuum is not polarized. The large attractive potential provided by the σ meson and the large repulsive potential provided by the ω meson naturally generate the spin-orbit potential, and therefore they lead to proper shell structures for finite nuclei without any additional parameters. The Dirac structure has more physical significance than it seems to have. For example, recently, the origin of the pseudospin symmetry has been naturally explained as a relativistic symmetry in the RMF model.[2),3)]

There are very few parameters in the RMF model, and all of them have clear

*) E-mail: lsgeng0@rcnp.osaka-u.ac.jp
**) E-mail: toki@rcnp.osaka-u.ac.jp
***) E-mail: mengj@pku.edu.cn

physical meanings. These parameters include the masses of the nucleons and the mesons and the coupling constants of the meson fields, and are usually fitted to the saturation properties of nuclear matter and the masses and charge radii of a few selected spherical nuclei. Based on such a simple physical picture, the RMF model has successfully described numerous nuclear properties in various regions: from stable nuclei[4] to unstable nuclei;[5)–7)] from the very light halo nucleus ^{11}Li[6] to the latest superheavy nucleus $^{288}115$;[8)] from neutron (proton) skins[9)] to proton emitters.[10)] Moreover, the successful descriptions of the anomalous kinks in the isotope shifts of Kr, Sr and Pb[11)] nuclei demonstrate that the RMF model can properly reproduce the deformations and the inherent shell effects of these nuclei, which altogether determine the anomalous kinks. However, these anomalous kinks are difficult to explain in the non-relativistic Hartree-Fock models. In addition to all these works on nuclear ground-state properties, there are equally many successful applications in other fields of nuclear physics, including identical bands in super-deformed nuclei,[12)] collective multipole excitations,[13)] hypernuclei,[14)] and neutron stars and supernovae,[15)] to name just a few.

Despite all the successes of the RMF model, a systematic study of all the nuclei throughout the periodic table from the proton drip line to the neutron drip line is still missing, due to several difficulties encountered in previous attempts. Firstly, a self-consistent calculation of the RMF model for deformed nuclei is very time consuming. Secondly, and more importantly, an efficient and economical pairing method that can treat all the nuclei from the proton drip line to the neutron drip line was not well known until recently. This is the reason that in 1997 Hirata et al. constructed a mass table for 2174 even-even nuclei with $8 \leq Z \leq 120$ without including the pairing correlation,[16)] and then, in 1999, Lalazissis et al. developed a mass table for 1315 even-even nuclei with $10 \leq Z \leq 98$ adopting a constant-gap BCS method.[17)]

In recent years, a state-dependent BCS method with a zero-range δ-force has been found to be an efficient and economical method to treat the pairing correlations for all the nuclei from the proton drip line to the neutron drip line.[18)–20)] This method not only can treat the continuum of neutron-rich nuclei reasonably well by taking into account the contribution of resonant states that have large overlaps with the occupied states below the Fermi surface, but also can avoid the problem of the convergence difficulty usually encountered in the constant-gap BCS method when moving away from the line of β stability. This method has been introduced into the axially-deformed RMF+BCS method,[20)] and it has been demonstrated to work well in almost the entire mass region.[8)–10),21)] With this method, we now are ready to perform a systematic study of the ground-state properties of all the nuclei with $Z, N \geq 8$ and $Z \leq 100$ from the proton drip line to the neutron drip line in the RMF model.

Such a systematic study is urgently needed, because experimentally, with developments in radioactive nuclear beams (RNB),[22)] more and more exotic nuclei can be investigated, and it is expected that more exotic phenomena, such as the so-called giant halos,[7)] will be discovered. Therefore, a theoretical model that can make reliable predictions, can successfully describe various new phenomena, and is also based on sound physical grounds is badly needed. Theoretically, to improve the present

formulation of the RMF model, to better understand its advantages and deficiencies, to get to know where and how to make further improvements, and finally to advance our understanding of nuclear structure, a systematic study of all the nuclei from the proton drip line to the neutron drip line within the RMF framework is needed.

This paper is organized as follows. First, we present the formulations and the numerical details in §2. Then, in §3, we compare the predictions of our calculations, including the binding energies, the separation energies, the deformations, and the charge radii, with existing experimental data, those of the finite-range droplet model (FRDM), and those of the Hartree-Fock-Bogoliubov (HFB) mass formula. The work is summarized in §4.

§2. Formulations and numerical details

The relativistic mean field (RMF) model has become a standard method to study nuclear properties. Therefore, here we only present the Lagrangian density adopted in the present work, which includes nonlinear terms for both the σ and ω mesons, and all the symbols have their usual meanings:

$$\begin{aligned}\mathcal{L} = & \bar{\psi}(i\gamma^\mu\partial_\mu - M)\psi \\ & + \frac{1}{2}\partial_\mu\sigma\partial^\mu\sigma - \frac{1}{2}m_\sigma^2\sigma^2 - \frac{1}{3}g_2\sigma^3 - \frac{1}{4}g_3\sigma^4 - g_\sigma\bar{\psi}\sigma\psi \\ & - \frac{1}{4}\Omega_{\mu\nu}\Omega^{\mu\nu} + \frac{1}{2}m_\omega^2\omega_\mu\omega^\mu + \frac{1}{4}g_4(\omega_\mu\omega^\mu)^2 - g_\omega\bar{\psi}\gamma^\mu\psi\omega_\mu \\ & - \frac{1}{4}R^a{}_{\mu\nu}R^{a\mu\nu} + \frac{1}{2}m_\rho^2\rho_\mu^a\rho^{a\mu} - g_\rho\bar{\psi}\gamma_\mu\tau^a\psi\rho^{\mu a} \\ & - \frac{1}{4}F_{\mu\nu}F^{\mu\nu} - e\bar{\psi}\gamma_\mu\frac{1-\tau_3}{2}A^\mu\psi. \end{aligned} \tag{2·1}$$

We use the parameter set TMA[23] for the mean-field Lagrangian density, which has proved to be one of the most successful modern parameter sets. The parameter values of the effective force TMA and the nuclear matter properties calculated with it are tabulated in Tables I and II. Here, it is worthwhile to note that the coupling constants of TMA are mass dependent. This originates from two other widely used parameter sets, TM1 and TM2.[23] In the process of developing a new parameter set to obtain better agreement for the behavior of the equation of state at high densities with that predicted by the relativistic Brueckner-Hartree-Fock theory, Sugahara and Toki realized that it is difficult to obtain good fits of heavy nuclei and light nuclei simultaneously using only one parameter set. For this reason, they developed TM1 for heavy nuclei and TM2 for light nuclei. Further studies led to the parameter set TMA, aiming at a consistent description of all the nuclei with one parameter set. From today's vantage point, the mass dependence of the coupling constants can be viewed as another form of density dependence. Recent studies indicate that the density dependence of the coupling constants, perhaps even the meson masses, may be needed to obtain a more satisfactory description of the experimental data, although the exact form of such a density dependence is presently under intense investigation.

Table I. Parameters of the effective force TMA.

	TMA
M_n	938.900 MeV
M_p	938.900 MeV
m_σ	519.151 MeV
m_ω	781.950 MeV
m_ρ	768.100 MeV
g_σ	$10.055 + 3.050/A^{0.4}$
g_ω	$12.842 + 3.191/A^{0.4}$
g_ρ	$3.800 + 4.644/A^{0.4}$
g_2	$-0.328 - 27.879/A^{0.4}$
g_3	$38.862 - 184.191/A^{0.4}$
g_4	$151.590 - 378.004/A^{0.4}$

Table II. Nuclear matter properties for the effective force TMA.

	TMA
ρ_{sat} (fm^{-3})	0.147
E_b (MeV)	-16.025
K (MeV)	318.146
J (MeV)	30.661
$M^*/M(n)$	0.635
$M^*/M(p)$	0.635

The RMF equations can be solved using the expansion method with the harmonic-oscillator basis.[4),20)] Fourteen shells are used for both the fermion fields and the meson fields, which have been tested and found capable of yielding reliable convergence in the region in question.

A zero-range δ-force, $V = -V_0\delta(\vec{r_1} - \vec{r_2})$, has been used in the particle-particle channel in order to achieve a consistent and reliable description for all the nuclei from the proton drip line to the neutron drip line. As usual, in this work the pairing strength is taken to be the same for both protons and neutrons, and it is obtained by fitting the experimental odd-even staggerings with the cutoff $E - \lambda \leq 8.0$ MeV, where E is the single-particle energy and λ the chemical potential. Due to the observed small variation of this quantity with the mass number A,[8),9),21)] we have used a mass-dependent formula for it, $V_0 = 300 + 120/A^{1/3}$, in order to obtain a consistent description for all the nuclei from the lightest ones to the heaviest ones. Except for the $A^{1/3}$ dependence,[24)] there are not many physical reasons for such a combination of coefficients. Also, we do not exclude the possibility that using a slightly different formula or adjusting it more carefully by dividing the entire periodic table into small areas can improve the final result somewhat. For nuclei with odd numbers of nucleons, a simple blocking method that does not break the time-reversal symmetry has been adopted.[9),21),25)]

In order to correctly locate the absolute minimum on the potential energy surface for each nucleus in the deformation space, a quadrupole-constrained calculation[26)] has been performed. We note that this is a rather time-consuming procedure, but

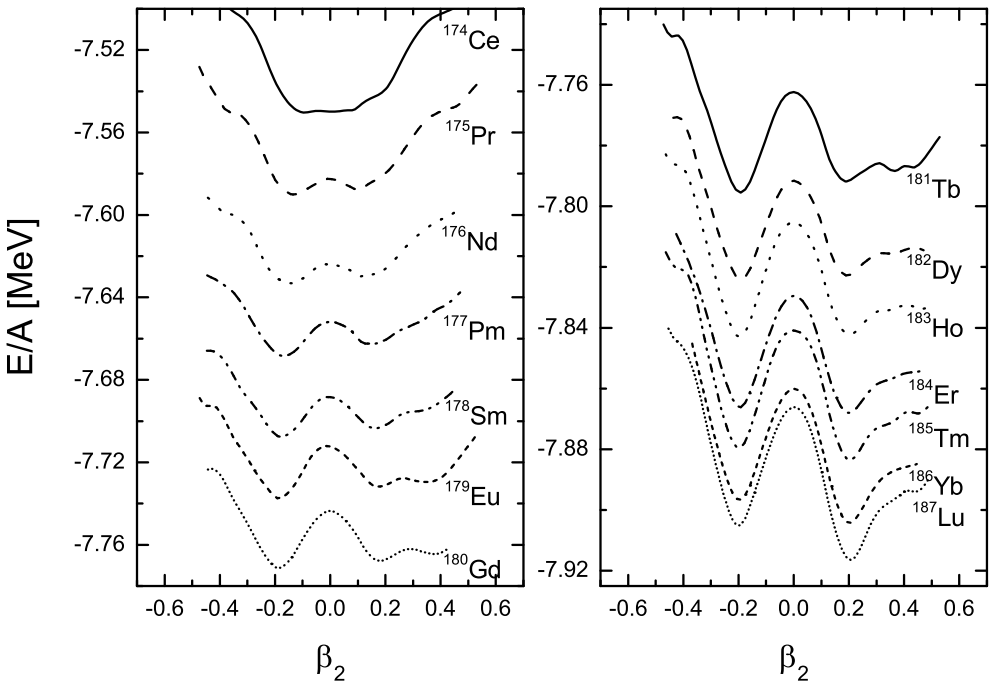

Fig. 1. The potential energy surfaces for 14 $N = 116$ isotones with $58 \leq Z \leq 71$, i.e ${}^{174}_{116}\mathrm{Ce}_{58}$, ${}^{175}_{116}\mathrm{Pr}_{59}$, ${}^{176}_{116}\mathrm{Nd}_{60}$, ${}^{177}_{116}\mathrm{Pm}_{61}$, ${}^{178}_{116}\mathrm{Sm}_{62}$, ${}^{179}_{116}\mathrm{Eu}_{63}$, ${}^{180}_{116}\mathrm{Gd}_{64}$, ${}^{181}_{116}\mathrm{Tb}_{65}$, ${}^{182}_{116}\mathrm{Dy}_{66}$, ${}^{183}_{116}\mathrm{Ho}_{67}$, ${}^{184}_{116}\mathrm{Er}_{68}$, ${}^{185}_{116}\mathrm{Tm}_{69}$, ${}^{186}_{116}\mathrm{Yb}_{70}$, and ${}^{187}_{116}\mathrm{Lu}_{71}$.

it is nevertheless necessary in order to find the ground-state configuration with the lowest energy for each nucleus. In Fig. 1, we display the energy per particle E/A for 14 $N = 116$ isotones with $58 \leq Z \leq 71$ in the rare-earth region as functions of the deformation parameter β_2. It is clearly seen how the deformation evolves as a function of the proton number Z: from a soft spherical shape to oblate, and then to a prolate shape as Z increases from 58 to 71.

We point out here that as a first attempt, neither the mean-field parameters nor the pairing-channel parameters adopted in this work have been constrained as stringently as those in most mass tables, such as FRDM[30] and HFB.[33] Therefore, the purpose of this work is not to obtain numbers that agree most closely with the measured experimental quantities but to obtain a fairly good description of the experimental data and gain some useful insight into the entire mass region in order to guide future works. Theoretically, the deviations from the experimental data can tell us a lot about the model itself. Some of the small deviations may be removed with finer adjustments of the parameters, and others may not. This will elucidate the need of going beyond the pure mean-field approximation and taking into account more high-order corrections. For similar reasons, we also ignore the rotational energy and the Wigner effect, which are more often treated by adding some phenomenological terms to the final total energy, except for the center-of-mass correction, which is

approximated by

$$E_{cm} = -\frac{3}{4}41A^{-\frac{1}{3}}. \tag{2·2}$$

We have also considered the contribution of the center-of-mass correction to the root-mean-square (rms) radii of the matter, proton and neutron density distributions:

$$\begin{aligned}
\delta\langle r_m^2\rangle &= -\frac{\langle r_m^2\rangle}{A}, \\
\delta\langle r_p^2\rangle &= -\frac{2\langle r_p^2\rangle}{A} + \frac{\langle r_m^2\rangle}{A}, \\
\delta\langle r_n^2\rangle &= -\frac{2\langle r_n^2\rangle}{A} + \frac{\langle r_m^2\rangle}{A}.
\end{aligned} \tag{2·3}$$

Altogether, the corrected rms radii of the matter, proton and neutron density distributions are

$$\begin{aligned}
R_m^2 &\equiv \langle r_m^2\rangle_{\rm corr} = \langle r_m^2\rangle + \delta\langle r_m^2\rangle, \\
R_p^2 &\equiv \langle r_p^2\rangle_{\rm corr} = \langle r_p^2\rangle + \delta\langle r_p^2\rangle, \\
R_n^2 &\equiv \langle r_n^2\rangle_{\rm corr} = \langle r_n^2\rangle + \delta\langle r_n^2\rangle.
\end{aligned} \tag{2·4}$$

For the rms charge radius, the finite size of the proton is taken into account by folding the point proton density distribution with a proton charge distribution of Gaussian type. This leads to

$$R_c^2 = R_p^2 + 0.64 \quad \text{fm}^2. \tag{2·5}$$

It should be noted that more effective methods exist for treating the finite size of the proton, but because the above-described method is that most often used in the literature, adopting such a prescription makes it easy to compare the results of our calculations with those of existing works. The same is also true for the center-of-mass correction to the total energy.[27)]

§3. Results and discussion

3.1. *Nuclear masses*

Making reliable and accurate predictions for nuclear masses over the entire periodic table has long been a major aim of nuclear physicists. (Recent reviews of this subject can be found in Ref.[28)]) Most related nuclear models can be classified into three categories. The first one consists of macroscopic models, such as the Bethe-Weizsäcker mass formula.[29)] The second one consists of the so-called macroscopic-microscopic models. One of the best in this category is the finite-range droplet model (FRDM).[30)] The last one consists of microscopic models, among which the best known are the Hartree-Fock (HF) method[31)] and the relativistic mean field model (RMF).[1)] The accuracy of one model is more or less determined by the number of parameters it employs and the procedure used to determine parameter values. For any given model, the more parameters used and/or the more quantities used

Table III. The rms deviations σ between theoretical predictions and experimental data[34] for nuclear masses. The second column contains the total number of experimental data considered in the comparison. The third through the fifth columns contain the rms deviations for the RMF+BCS model, the FRDM mass formula,[30] and the HFB-2 mass formula,[33] respectively. All energies are in units of MeV.

Group	number	σ(RMF+BCS)	σ(FRDM)	σ(HFB-2)
I	2882	2.118	0.791	0.843
II	2157	2.108	0.626	0.739
III	1960	2.107	0.617	0.735

to determine the parameters, the more accurate it should be. By the latter means, the agreement of the predictions of the Hartree-Fock method with experimental nuclear masses has recently been increased to the same level as those of the FRDM mass formula.[32),33)] Comparing the numbers of parameters of different models is less meaningful, but usually it is believed that the more microscopic a model, the more reliable it should be when extrapolated to unknown areas that have not yet been fitted. In this respect, it is generally accepted that the RMF model is one of the most promising, due to its explicit Lorentz invariance.

One of the quantities often used to describe the overall agreement of the theoretical predictions and the experimental masses is the root-mean-square (rms) deviation σ, defined by

$$\sigma = \sqrt{\frac{\sum_{i=1}^{N} \left(M^i_{\rm theo} - M^i_{\rm exp}\right)^2}{N}}, \tag{3·1}$$

where N is the total number of experimental data. In Table III, we tabulate this quantity for our calculations, the FRDM mass formula,[30] and the HFB-2 mass formula.[33] The FRDM and HFB-2 mass formulae have been elegantly constructed by fitting their parameters to masses of more than 1000 known nuclei. Therefore, their rms deviations σ can be considered the lower limit that any phenomenological model can achieve. (To be precise, the current lower limit of σ for the mass formula is about 0.3 MeV.[28]) In order to remove the influence of the experimental errors, we divide all the 2882 nuclear masses with $Z, N \geq 8$ and $Z \leq 100$ compiled in Audi 2003[34] into three groups. The first group, Group I, includes all the nuclei without any restrictions on their experimental errors. It contains 2882 nuclei. The second group, Group II, includes those nuclei whose experimental errors are less than 0.2 MeV. It contains 2157 nuclei. The last group, Group III, includes only those nuclei whose experimental errors are less than 0.1 MeV. It contains 1960 nuclei. Here it should be noted that not all the 2882 nuclear masses are experimental data. Some of them are extrapolated data using "systematic trends".[34] However, due to the fact that these data are usually very close to the experimental data,[28] we do not make any distinction here.

Two things can be learned from Table III. First, the FRDM mass formula, which is the oldest, exhibits the best agreement with the experiment results, while our calculation has the largest σ. The HFB-2 mass formula is similar to the FRDM

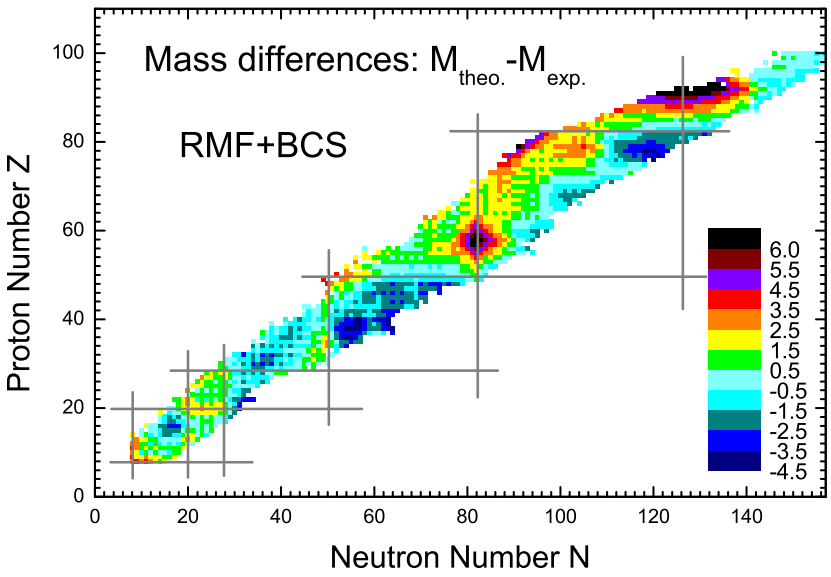

Fig. 2. Mass differences between the predictions of the present work and the experimental data for 2157 nuclei whose measured uncertainties for the masses are less than 0.2 MeV.[34)]

mass formula, with its σ being about 0.1 MeV larger than that of the FRDM mass formula. However, noting that both FRDM and HFB-2 used more than 1000 nuclear masses to fit their parameters, it is fair to say that our results are fairly good. The second point here is that the σ of the FRDM mass formula changes most when going from the third group to the first group. The reason for this is not clear, because the TMA parameter set is almost as old as that of the FRDM mass formula. The σ of the HFB-2 mass formula also changes about 0.1 MeV, compared to 0.01 MeV for our calculations.

To have a much clearer picture of the physics behind σ, we plot the mass differences between the results of our calculations and the experimental data for all the nuclei of Group II in Fig. 2. We have chosen Group II so that the data set is not too small and the experimental error is not too large to undermine the analysis. (From this point, we always use the experimental masses of Group II to make comparisons.) There are several interesting things that can be learned immediately from this figure, as discussed below:

1. Most deviations are in the range of -2.5-2.5 MeV, which explains our overall rms deviation of $\sigma \approx 2.1$ MeV.
2. There are several strongly overbound regions. The first one is near $Z = 92$ and $N = 126$, the second one is near $Z = 58$ and $N = 82$, and the third one is near $Z = 78$ and $N = 92$. Although the experimental data do exhibit some signs of the magic nature of these nuclei, apparently, the present RMF model somewhat overestimates the effect of their magic properties. We stress that these discrepancies exist not only in the present calculation but also in all the

other modern RMF calculations, regardless of the parameter sets and other details.

3. In the $Z \geq 50$ region, along a certain isotopic chain, the proton-rich side is usually overestimated, while the neutron-rich side is usually underestimated. The two exceptions are near $(Z = 58, N = 82)$ and in the upper-right corner of the figure. The behavior of other parameter sets including the latest ones indicates that this is common to almost all the existing parameter sets.[35)]
4. There are also areas where there seems to be strong underbinding. One is near $Z = 38$ and $N = 60$, where prolate and oblate shapes are found to coexist (see Fig. 3). The other region is near $Z = 78$ and $N = 120$.
5. More nuclei with $Z \geq 50$ seem to be overestimated, while more nuclei with $28 < Z < 50$ seem to be underestimated somewhat.

We believe that a more extensive study of all these deviations will clarify whether it is simply a matter of model parameters or that the pure RMF model itself is too simple to account for all the underlying physics and therefore that higher-order corrections need to be introduced. Investigations to clarify this point are in progress.

One might be tempted to argue that the general underbinding for nuclei with $28 < Z < 50$ and the general overbinding for nuclei with $Z > 50$ could be compensated for by adjusting the pairing strength more carefully. Of course, this may work to some extent. But the problem is not really that simple, because on the one hand, the pairing correlations are not large enough to compensate for all the deviations (particularly the overbinding part), and on the other hand, the pairing correlations should not be that complicated. (The most complicated pairing strength ever used in the zero-range pairing method known to us is that adopted in the works of Goriely et al.,[32),33)] which is slightly different for protons and neutrons and also depends on whether the number of nucleons is even or odd.) A more reasonable explanation is that the shell structure is somewhat incorrect and the coexistence of prolate and oblate shapes (see discussion below).

There is one more difference between the results of the RMF+BCS, FRDM and HFB-2 calculations. It is found that although these three models predict similar results near the line of β stability, their results are quite different for heavy neutron-rich nuclei. Neutron drip-line nuclei in the RMF+BCS calculation are found to be more strongly bound (by about 20 MeV) than those in HFB-2, while those in HFB-2 are also more strongly bound (by about 20 MeV) than those in FRDM. These features should be checked by experiments with the new generation of radioactive ion beam facilities.

3.2. *Separation energies*

Compared to the nuclear masses, the one-neutron and two-neutron separation energies are more important in investigating the nuclear shell structures and less dependent on the finer adjustment of the model parameters, because systematic errors can be cancelled somewhat by subtraction. In Table IV, we tabulate the rms deviations of the one-neutron separation energies for our results, for those obtained from the FRDM mass formula, and for those obtained from the HFB-2 mass formula. One thing that needs to be noted here is that the experimental error is that of the

Table IV. The same as Table III, but for the one-neutron separation energies.

Group	number	σ(RMF+BCS)	σ(FRDM)	σ(HFB-2)
I	2790	0.667	0.437	0.509
II	1994	0.640	0.372	0.466
III	1767	0.638	0.369	0.466
IV	1030	0.673	0.393	0.506

one-neutron separation energies, not that of the nuclear masses, so now the number of nuclei in each group is smaller than that appearing in Table III. Because the experimental error can more strongly influence σ in this situation, we add another group (Group IV), which includes only those nuclei for which the experimental error of the one-neutron separation energies is less than 0.02 MeV.

Most conclusions we derive from the study of the nuclear masses still hold: The FRDM has the best agreement with experiment, the HFB-2 is a little worse, and ours still has the largest deviation, except that now the difference between our calculations and those of the other two nonrelativistic models has been reduced by about half. That is to say, for the one-neutron separation energies, our calculations are similar to those employing the other two mass formulae. Because in most practical applications, differential quantities, such as the one-neutron separation energies, are of more interest than the absolute nuclear masses, this makes our results comparable to those of the FRDM and HFB-2 mass formulae.

3.3. *Deformations*

The RMF model with modern parameter sets can reproduce the deformations of finite nuclei very well, particularly those of the rare-earth nuclei.[36] Experimentally, only for a few even-even nuclei, deformation parameters can be extracted from the experimental $BE(2)$ values.[37] However, an overall σ like those used in treating the nuclear masses and the separation energies will be less useful, because on the one hand, it is a small quantity with an absolute value less than 1, and on the other hand, the empirical uncertainty is relatively large. What are more interesting are the overall general features exhibited by different models. To see this, we plot the proton quadrupole deformation parameters for all the nuclei with Z, $N \geq 8$ and $Z \leq 100$ from the three different models, RMF+BCS, FRDM and HFB-2, in Fig. 3. The following conclusions can be readily drawn.

1. Only very few nuclei are strictly spherical ($-0.05 \leq \beta_{2p} \leq 0.05$) and most of them are located at or near the magic numbers. While RMF+BCS and FRDM exhibit only small numbers of spherical nuclei, HFB-2 exhibits a large number: More nuclei near the magic numbers are spherical in the HFB-2 mass formula than in the other two models. This can be seen quite clearly from Fig. 3.
2. While isotonic chains with neutron magic numbers ($N = 82, 126, 184$) seem to preserve spherical shapes for the entire chains, isotopic chains with proton magic numbers are usually deformed when one moves away from the neutron magic numbers (except for the $Z = 20$ isotopic chain). Among the three models we employed here, RMF+BCS and FRDM display this feature clearly, while

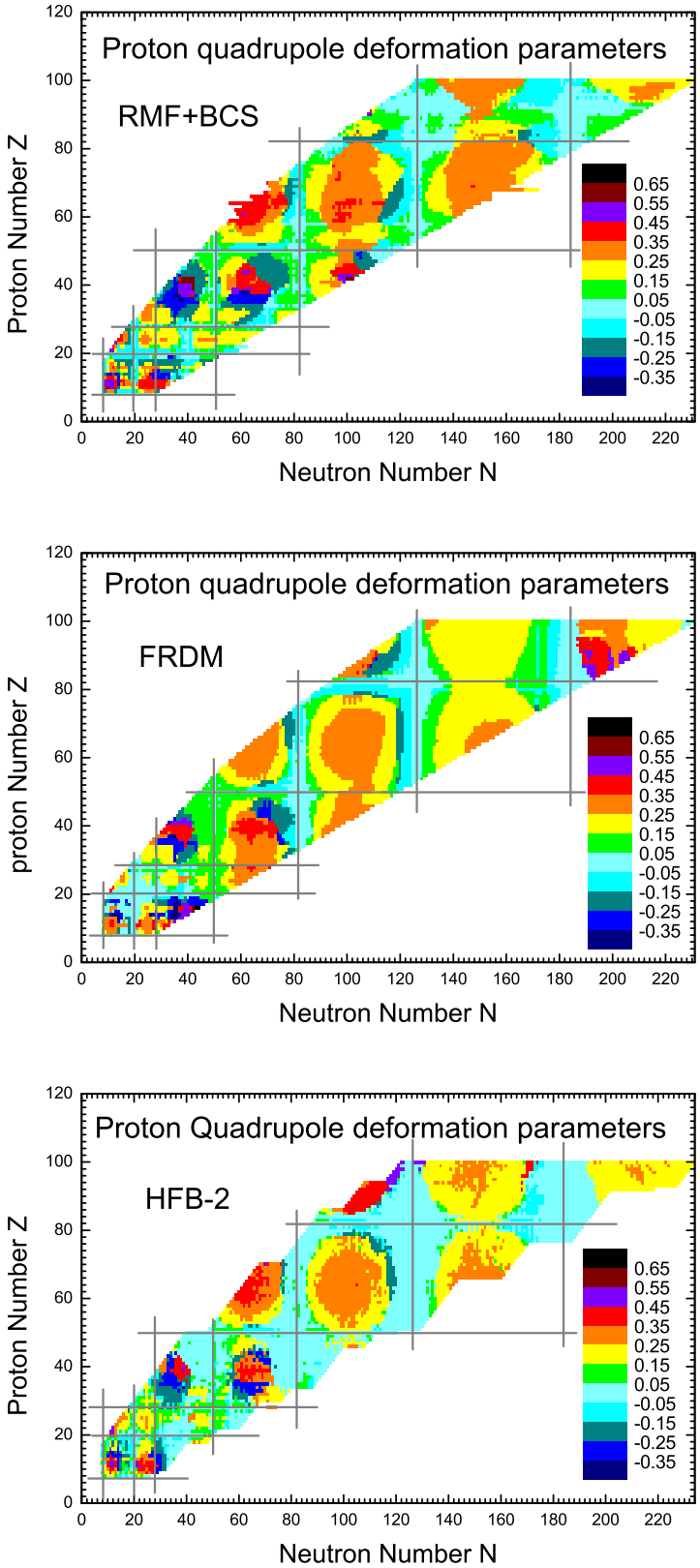

Fig. 3. The proton quadrupole deformation parameters, β_{2p}, for 2157 nuclei whose measured uncertainties for masses are less than 0.2 MeV.[34] The data obtained in the RMF+BCS calculations, the FRDM mass formula,[30] and the HFB-2 mass formula[33] are displayed in the top, middle, and bottom panels, respectively.

HFB-2 predicts a large number of spherical nuclei, as discussed above.

3. Most nuclei with $Z > 50$ become prolate deformed when moving away from the magic numbers either isotonically or isotopically and have the largest deformations in the middle of major shells. When approaching the magic neutron number from the lower-N side, a transition from moderately prolate shapes to moderately oblate shapes seems to occur often.
4. There are also several regions where strongly prolate and oblate deformations coexist. The first is near $28 < Z < 50$ and $28 < N < 50$. The second is near $28 < Z < 50$ and $50 < Z < 82$. If we recall what we have found in the study of the nuclear masses, we note that these regions are where the nuclear masses are a bit underestimated in our calculations. There seem to be some connections between these two phenomena: shape coexistence and underbinding. Since shape coexistence usually implies the existence of a triaxial deformation, extra degrees of freedom in the deformation space might be needed to better describe these nuclei.
5. Another region where prolate and oblate shapes coexist is near $8 < Z < 20$ and $8 < N < 20$. The other is near $8 < Z < 20$ and $28 < N < 50$. The FRDM model exhibits the latter one more clearly.
6. Except for the common features exhibited by all the three models studied above, there are some features unique to individual models. One is that FRDM exhibits strong deformation (prolate) in the upper-right corner of the $(Z = 82, N = 184)$ intersection, while the other two models predict more or less spherical shapes in this region. This difference is interesting for two reasons. First, it represents a difference between macroscopic-microscopic models and microscopic models. Second, it influences the magic nature of $Z = 82$ and $N = 184$. Another feature unique to HFB-2 is that it exhibits a strong prolate deformation in the upper-left corner of the $(Z = 82, N = 126)$ intersection.
7. We found in the above investigation of the nuclear masses that the regions $(Z \approx 92, N \approx 126)$ and $(Z \approx 58, N \approx 82)$ exhibit the general feature of overbinding for the case of the RMF model. The same situation is found here. Looking at Fig. 3, it is easily seen that there is another isotopic chain, with $Z = 92$, exhibiting the feature (having more spherical nuclei) of conventional proton magic numbers. The same is also true for $Z = 58$, whose magic nature is especially conspicuous in the two regions near $N = 82$ and $N = 126$.

To summarize, the general features for the nuclear deformations exhibited by our calculations are supported by the other two mass formulae. We also note that there seem to be close connections between the two nuclear properties, nuclear masses and deformations. Anomalies appearing in one plot (Fig. 2) can often be found in the other (Fig. 3) in one way or another. This provides an interesting way to locate the anomalies and to understand the underlying physics that causes them. The several regions in which underbinding exists in connection with shape coexistence are very good candidates to study the possibility of triaxial deformations.

3.4. *Charge radii*

In addition to the nuclear deformations, the root-mean-square (rms) charge radii are also very important quantities to describe the shapes of finite nuclei. In Table V, we tabulate the rms deviations of our data from the empirical data compiled by Nadjakov et al.[38] for 523 nuclei in 42 isotopic chains. For comparison, the corresponding quantities for the calculations of the FRDM and HFB-2 mass formulae are also shown.

We can learn several things from Table V. First, the overall value of σ for the 523 nuclei in our calculations (0.037 fm) is just the average of that of the FRDM mass formula (0.045 fm) and that of the HFB-2 mass formula (0.028 fm). Considering the fact that our parameters are not constrained as stringently as either of the other two mass formulae, this result is acceptable, though further improvements are expected. In fact, our results are even closer to the empirical data in the rare-earth region than those of the HFB-2 mass formula. Second, there are several isotopic chains for which σ is larger than 0.05 fm, including $Z = 11$, $Z = 38$, $Z = 46$, $Z = 78$, $Z = 79$, $Z = 80$, $Z = 90$ and $Z = 94$. Recalling our discussion of the nuclear masses and the deformations, we note that these are either the magicity-overestimated or prolate-oblate-coexisting regions.

Although not shown here, the much discussed kink in the charge radii of Pb isotopes can be reproduced very well with our present calculations, as with almost all the RMF calculations,[35] while all the Hartree-Fock calculations,[32),33] though very successful in reproducing the nuclear masses, have failed in this respect.

Another difference between our calculations and those of the HFB-2 mass formula for the nuclear charge radii is that our results are generally larger than those of HFB-2 by 0.05-0.15 fm for heavy neutron-rich nuclei with $Z > 50$. Not only the absolute charge radii but also the neutron-skin thickness defined as $\theta_n = R_n - R_p$, where R_n and R_p are the rms neutron and proton radii, is found to be somewhat larger than its HF counterpart. The neutron skin of ^{208}Pb in our calculations is 0.26 fm, while the HFB-2 mass formula predicts 0.12 fm.[33] Recent experimental results include 0.20 ± 0.04 fm,[40] 0.19 ± 0.09 fm,[41] and 0.17 fm (no uncertainties given).[42] Due to the large experimental uncertainties, more experimental data are needed before any firm conclusion can be drawn. It is worthwhile to note that for ^{208}Pb, $\theta_n = 0.26$ fm and $\theta_n = 0.12$ fm are two typical values in the RMF model and in the HF model.[43] The relation between this quantity and the density-dependence of the symmetry energy is presently under active investigation.[43] We will study this elsewhere.[44]

§4. Summary

We have performed a systematic study of 6969 nuclei with $Z, N \geq 8$ and $Z \leq 100$ from the proton drip line to the neutron drip line in the relativistic mean field model. Comparisons with two of the most successful existing mass formulae, FRDM and HFB-2, have been made. Reasonable agreement with the available experimental data is realized for the nuclear masses, the separation energies, and the rms charge

Table V. The rms deviations σ between theoretical predictions and empirical data[38] for the rms charge radii. The first column labels the isotopic chains and the second column the number of isotopes in each chain. Columns 3, 4, and 5 are from the RMF+BCS calculations, the FRDM mass formula,[30] and the HFB-2 mass formula,[33] respectively. The data for the FRDM mass formula are taken from Ref.[39] All radii are in units of fm.

Z	number	σ(RMF+BCS)	σ(FRDM)	σ(HFB-2)
11	12	0.053	0.151	0.056
19	10	0.031	0.093	0.011
20	10	0.041	0.091	0.023
24	4	0.025	0.088	0.006
28	5	0.024	0.081	0.010
36	8	0.024	0.037	0.027
38	22	0.056	0.082	0.025
40	5	0.025	0.063	0.010
42	7	0.021	0.047	0.029
44	7	0.029	0.033	0.036
46	6	0.053	0.070	0.019
47	6	0.007	0.034	0.020
48	17	0.023	0.022	0.042
49	24	0.025	0.015	0.038
50	18	0.008	0.035	0.015
54	20	0.016	0.033	0.015
55	29	0.014	0.035	0.015
56	28	0.010	0.029	0.016
57	3	0.003	0.026	0.004
58	4	0.003	0.019	0.014
60	16	0.006	0.024	0.017
62	17	0.007	0.013	0.025
63	22	0.020	0.012	0.031
64	8	0.013	0.011	0.017
66	18	0.015	0.009	0.033
67	14	0.025	0.023	0.013
68	12	0.011	0.006	0.026
69	17	0.044	0.047	0.033
70	18	0.011	0.009	0.022
71	4	0.044	0.054	0.058
72	7	0.010	0.009	0.006
74	5	0.024	0.015	0.009
76	7	0.034	0.008	0.017
78	14	0.104	0.067	0.034
79	15	0.068	0.021	0.025
80	26	0.056	0.025	0.031
81	18	0.029	0.018	0.012
82	22	0.028	0.015	0.019
90	5	0.054	0.065	0.048
92	5	0.027	0.023	0.024
94	6	0.070	0.016	0.021
95	2	0.030	0.028	0.021
	523	0.037	0.045	0.028

radii. The general features of the nuclear deformations were studied together with those exhibited by the FRDM and HFB-2 mass formulae. Several regions in which the deviations from the experimental data seem a bit large have been pointed out, and possible factors causing them have been discussed.

The overall σ of 2.1 MeV for the nuclear masses, though better than the previous RMF calculation[17] (2.8 MeV), is still not satisfactory. Based on the present work, further improvements should be made in order to make the predicted nuclear masses satisfy the precision required for astrophysical studies. Possible promising directions include adjusting the parameter values of the mean-field channel and the pairing channel together, taking into account the residual corrections ignored in this work, including the rotational energy and the Wigner effect, and restoring the broken gauge symmetry of the particle number. Another possibility is to replace the harmonic-oscillator basis with the woods-saxon basis in order to make the calculations for neutron-rich nuclei more reliable.[45]

A complete calculation that includes all the higher-order correlations mentioned above is still not very likely in the near future in the relativistic mean field model. Therefore, our present study should be seen as a first attempt in this direction rather than the final work. All future works should first find how to reduce the overestimated magicities in the several areas that we discussed. Also, triaxial degrees of freedom might be needed in the several regions where our study indicates possible shape coexistence. In this respect, a systematic study of all the nuclei throughout the periodic table will be very helpful for all future works along this direction. A more detailed study of the results of the present calculation is in progress.

References

1) J. D. Walecka, Ann. of Phy. **83** (1974), 491.
   B. D. Serot and J. D. Walecka, Adv. Nucl. Phys. **16** (1986), 1.
   P. G. Reinhard, Rep. Prog. Phys. **52** (1989), 439.
   P. Ring, Prog. Part. Nucl. Phys. **37** (1996), 193.
2) J. Ginocchio, Phys. Rev. Lett. **78** (1997), 436.
   J. N. Ginocchio, A. Leviatan, J. Meng and Shan-Gui Zhou, Phys. Rev. C **69** (2004), 034303.
3) J. Meng, K. Sugawara-Tanabe, S. Yamaji, P. Ring and A. Arima, Phys. Rev. C **58** (1998), 628(R).
   J. Meng, K. Sugawara-Tanabe, S. Yamaji and A. Arima, Phys. Rev. C **59** (1999), 154.
4) Y. K. Gambhir, P. Ring and A. Thimet, Ann. of Phys. **198** (1990), 132.
5) D. Hirata, H. Toki, T. Watabe, I. Tanihata and B. S. Carlson, Phys. Rev. C **44** (1991), 1467.
6) J. Meng and P. Ring, Phys. Rev. Lett **77** (1996), 3963.
7) J. Meng and P. Ring, Phys. Rev. Lett **80** (1998), 460.
   J. Meng, H. Toki, J. Y. Zeng, S. Q. Zhang and S.-G. Zhou, Phys. Rev. C **65** (2002), 041302(R).
8) L. S. Geng, H. Toki and J. Meng, Phys. Rev. C **68** (2003), 061303(R).
9) L. S. Geng, H. Toki, A. Ozawa and J. Meng, Nucl. Phys. A **730** (2004), 80.
10) L. S. Geng, H. Toki and J. Meng, Prog. Theor. Phys. **112** (2004), 603.
11) M. M. Sharma, G. A. Lalazissis and P. Ring, Phys. Lett. B **317** (1993), 9.
    G. A. Lalazissis and M. M. Sharma, Nucl. Phys. A **586** (1995), 201.
12) J. König and P. Ring, Phys. Rev. Lett. **71** (1993), 3079.
13) Z.-Y. Ma, A. Wandelt, N. V. Giai, D. Vretenar, P. Ring and L.-G. Gao, Nucl. Phys. A **703** (2002), 222.
14) H. F. Lü, J. Meng, S. Q. Zhang and S.-G. Zhou, J. Eur. Phys. A **17** (2003), 19.

15) H. Shen, H. Toki, K. Oyamatsu and K. Sumiyoshi, Nucl. Phys. A **637** (1998), 435.
H. Shen, Phys. Rev. C **65** (2002), 035802.
16) D. Hirata, K. Sumiyoshi, I. Tanihata, Y. Sugahara, T. Tachiba and H. Toki, Nucl. Phys. A **616** (1997), 438c.
17) G. A. Lalazissis, S. Raman and P. Ring, At. Data. Nucl. Data Tables **71** (1999), 1.
18) N. Sandulescu, Nguyen Van Giai and R. J. Liotta, Phys. Rev. C **61** (2000), 061301(R).
M. Grasso, N. Sandulescu, Nguyen Van Giai and R. J. Liotta, Phys. Rev. C **64** (2001), 064321.
19) H. L. Yadav, S. Sugimoto and H. Toki, Mod. Phys. Lett. A **17** (2002), 2523.
N. Sandulescu, L. S. Geng, H. Toki and G. C. Hillhouse, Phys. Rev. C **68** (2003), 054323.
20) L. S. Geng, H. Toki, S. Sugimoto and J. Meng, Prog. Theor. Phys. **110** (2003), 921.
21) L. S. Geng, H. Toki and J. Meng, Mod. Phys. Lett. A **19** (2004), 2171.
22) I. Tanihata, Prog. Part. Nucl. Phys. **35** (1995), 505.
A. Mueller, Prog. Part. Nucl. Phys. **46** (2001), 359.
23) Y. Sugahara and H. Toki, Nucl. Phys. A **579** (1994), 557.
Y. Sugahara, Ph.D. thesis, Tokyo Metropolitan University, 1995.
24) W. Satula, J. Dobaczewski and W. Nazarewicz, Phys. Rev. Lett **81** (1998), 3599.
S. Hilaire, J. F. Berger, M. Girod, W. Satula and P. Schuck, Phys. Lett. B **531** (2002), 61.
25) P. Ring and P. Schuck, *The Nuclear Many-Body Problem* (Springer, 1980).
26) H. Flocard, P. Quentin, A. K. Kerman and D. Vautherin, Nucl. Phys. A **203** (1973), 433.
27) M. Bender, K. Rutz, P.-G. Reinhard and J. A. Maruhn, Eur. Phys. J. A **7** (2000), 467.
28) D. Lunney, J. M. Pearson and C. Thibault, Rev. Mod. Phys. **75** (2003), 1021.
29) K. Heyde, *Basic Idears and Concepts in Nuclear Physics* (IOP, 1999).
30) P. Möller, J. R. Nix, W. D. Myers and W. J. Swiatecki, At. Data Nucl. Data Tables **59** (1995), 185.
P. Möller, J. R. Nix and K.-L. Kratz, At. Data Nucl. Data Tables **66** (1997), 131.
31) T. H. R. Skyrme, Phil. Mag. **1** (1956), 1043.
J. Dechargé and D. Gogny, Phys. Rev. C **21** (1980), 1568.
H. Flocard, P. Quentin and D. Vautherin, Phys. Lett. B **46** (1973), 304.
32) S. Goriely, F. Tondeur and J. M. Pearson, At. Data Nucl. Data Tables **77** (2001), 311.
33) M. Samyn, S. Goriely, P.-H. Heenen, J. M. Pearson and F. Tondeur, Nucl. Phys. A **700** (2002), 142.
S. Goriely, M. Samyn, P.-H. Heenen, J. M. Pearson and F. Tondeur, Phys. Rev. C **66** (2002), 024326.
M. Samyn, S. Goriely and J. M. Pearson, Nucl. Phys. A **725** (2003), 69.
S. Goriely, M. Samyn, M. Bender and J. M. Pearson, Phys. Rev. C **68** (2003), 054325.
34) G. Audi, A. H. Wapstra and C. Thibault, Nucl. Phys. A **729** (2003), 337.
35) Wenhui Long, Jie Meng, Nguyen Van Giai and Shan-Gui Zhou, Phys. Rev. C **69** (2004), 034319.
36) G. A. Lalazissis, M. M. Sharma and P. Ring, Nucl. Phys. A **597** (1996), 35.
T. Nǐksić, D. Vretenar, G. A. Lalazissis and P. Ring, Phys. Rev. C **69** (2004), 047301.
37) S. Raman, C. W. Nestor, JR. and P. Tikkanen, At. Data Nucl. Data Tables **78** (2001), 1.
38) E. G. Nadjakov, K. P. Marinova and Yu. P. Gangrsky, At. Data. Nucl. Data Tables **56** (1994), 133.
39) F. Buchinger, J. M. Pearson and S. Goriely, Phys. Rev. C **64** (2001), 067303.
40) V. E. Starodubsky and N. M. Hintz, Phys. Rev. C **49** (1994), 2118.
41) A. Krasznahorkay et al., Nucl. Phys. A **567** (1994), 521.
42) S. Karataglidis, K. Amos, B. A. Brown and P. K. Deb, Phys. Rev. C **65** (2002), 044306.
43) B. Alex Brown, Phys. Rev. Lett. **85** (2000), 5296.
S. Typel and B. Alext Brown, Phys. Rev. C **64** (2001), 027302.
C. J. Horowitz and J. Piekarewicz, Phys. Rev. Lett. **86** (2001), 5647.
C. J. Horowitz and J. Piekarewicz, Phys. Rev. C **64** (2001), 062802 (R).
44) L. S. Geng, H. Toki and J. Meng, in preparation.
45) S.-G. Zhou, J. Meng and P. Ring, Phys. Rev. C **68** (2003), 034323.